



OPEN ACCESS

EDITED BY

Arun K. Bhunia,
Purdue University, United States

REVIEWED BY

Shanshan Wang,
Chinese Academy of Agricultural Sciences,
China

Hui-Wen Gu,
Yangtze University, China

*CORRESPONDENCE

Zhen-Lin Xu

✉ jallent@163.com

Hongwu Wang

✉ hwwang@zqu.edu.cn

RECEIVED 13 October 2023

ACCEPTED 04 December 2023

PUBLISHED 21 December 2023

CITATION

Chen Z-J, Huang A-J, Dong X-X, Zhang Y-F,
Zhu L, Luo L, Xu Z-L and Wang H (2023) A
simple and sensitive fluoroimmunoassay
based on the nanobody-alkaline phosphatase
fusion protein for the rapid detection of
fenitrothion.

Front. Sustain. Food Syst. 7:1320931.

doi: 10.3389/fsufs.2023.1320931

COPYRIGHT

© 2023 Chen, Huang, Dong, Zhang, Zhu,
Luo, Xu and Wang. This is an open-access
article distributed under the terms of the
[Creative Commons Attribution License
\(CC BY\)](https://creativecommons.org/licenses/by/4.0/). The use, distribution or reproduction
in other forums is permitted, provided the
original author(s) and the copyright owner(s)
are credited and that the original publication
in this journal is cited, in accordance with
accepted academic practice. No use,
distribution or reproduction is permitted
which does not comply with these terms.

A simple and sensitive fluoroimmunoassay based on the nanobody-alkaline phosphatase fusion protein for the rapid detection of fenitrothion

Zi-Jian Chen^{1,2,3}, Ai-Jun Huang^{1,2,3}, Xiu-Xiu Dong⁴,
Yi-Feng Zhang⁵, Lin Zhu⁶, Lin Luo⁵, Zhen-Lin Xu^{5*} and
Hongwu Wang^{1,2,3*}

¹School of Food & Pharmaceutical Engineering, Zhaoqing University, Zhaoqing, China, ²Laboratory of Quality & Safety Risk Assessment for Agro-Products (Zhaoqing), Ministry of Agriculture and Rural Affairs, Zhaoqing, China, ³Guangdong Engineering Technology Research Center of Food & Agricultural Product Safety Analysis and Testing, Zhaoqing, China, ⁴Key Laboratory of Modern Agricultural Equipment and Technology (Jiangsu University), Ministry of Education, School of Agricultural Engineering, Jiangsu University, Zhenjiang, China, ⁵Guangdong Provincial Key Laboratory of Food Quality and Safety, South China Agricultural University, Guangzhou, China, ⁶Guangzhou Experimental Station, Chinese Academy of Tropical Agricultural Sciences, Guangzhou, China

Immunoassay is a powerful tool for the rapid detection of small harmful organic molecules. In this study, a simple and sensitive fluoroimmunoassay (FIA) based on a nanobody-alkaline phosphatase fusion protein (VHHjd8-ALP) and blue-emissive carbon dots (bCDs) was developed for the rapid detection of fenitrothion. The bCDs were synthesized using the one-step hydrothermal method. Citric acid and urea were used as carbon and nitrogen sources, respectively. The synthesized bCDs were characterized by fluorescence spectrum, high-resolution transmission electron microscopy, x-ray photoelectron spectroscopy, and Fourier transform infrared spectroscopy. After one step of competitive immunoassay, the VHHjd8-ALP bound to the microplate and catalyzed the substrate p-nitrophenylphosphate (pNPP) into p-nitrophenol (pNP); the latter can quench the blue of bCDs due to an inner-filter effect. After condition optimization, an FIA calibration curve was finally created, which showed an IC₅₀ value of 16.25 ng/mL and a limit of detection (LOD) of 0.19 ng/mL. Compared with the pNPP-based one-step conventional indirect competitive enzyme-linked immunoassay (icELISA), the developed FIA showed an 11-fold sensitivity improvement. Furthermore, the analysis period of FIA only takes approximately 55 min, which was obviously faster than that of the conventional icELISA. The recovery test showed recoveries from 81.8 to 119% with fruits and vegetable samples, which verified the practicability and accuracy of the developed FIA.

KEYWORDS

fluoroimmunoassay, fenitrothion, carbon dots, nanobody-alkaline phosphatase fusion protein, rapid detection

Introduction

Pesticide is indispensable for modern agriculture. However, the improper and excessive use of pesticides results in residues in foods and environments, which is a serious problem. Furthermore, consuming foods with high pesticide residue levels over the recommended levels can cause chronic poisoning and even cancer (Yang et al., 2018; Pedroso et al., 2022). Fenitrothion is a highly effective organophosphorus insecticide with a broad spectrum of activity. It is extensively utilized for controlling a wide range of pests and is also employed for the management of flies, mosquitoes, and other disease-carrying vectors, thereby contributing to the prevention of malaria and other public health issues (Gnanguenon et al., 2015; Abdel-Ghany et al., 2016). However, previous studies showed that the fenitrothion was harmful to human beings through the inhibition of the acetylcholinesterase activity (Faria et al., 2022). Moreover, fenitrothion exposure was associated with hepatic injury, renal injury, and reproductive toxicity (Galal et al., 2019; Li et al., 2023). As a consequence, the amount of fenitrothion residues in foods should be strictly monitored.

For the detection of fenitrothion, several methods have been reported in previous studies, including high-performance liquid chromatography (HPLC) (Ulusoy et al., 2020), gas chromatography–mass spectrometry (GC–MS/MS) (Kang et al., 2020), electrochemical sensor (Han et al., 2023), and fluorescent sensor (Delnavaz et al., 2023). However, fenitrothion is detected primarily through instrumental analysis, which is expensive, requires professional operators, and takes a long time. Therefore, it is necessary to develop a rapid, simple, sensitive, and low-cost method for the detection of fenitrothion.

Immunoassay is a powerful detection tool in analytical chemistry and exhibits broad applicability for accurately quantifying analytes present at extremely low concentrations (Wang et al., 2022), which shows advantages of sensitivity, rapid, high specificity, low cost, and easy-to-use. Conventional immunoassay depends on the output of the colorimetric signal, which limits the sensitivity for analysis. As an alternative, fluoroimmunoassay (FIA) is a promising and powerful detection tool owing to its advantages such as high sensitivity, non-destructive characteristics, real-time, fast response, and low cost (Yi et al., 2020). For the development of FIA, the fluorescent probe is the key element for signal amplification. As a novel fluorescent nanomaterial, carbon dots (CDs) show excellent features such as wide sources, cost-effectiveness, low toxicity, water-solubility, and easy synthesis (Luo et al., 2013; Lee et al., 2016; Zhu et al., 2019; Lin et al., 2021), which have garnered growing interest and are considered excellent candidates for the development of FIA.

In this study, an anti-fenitrothion nanobody-alkaline phosphatase fusion protein (VHHjd8-ALP) was employed to develop CDs-based FIA. As shown in Scheme 1, in the absence of fenitrothion, the VHHjd8-ALP binds on the microplate after a one-step competitive immunoassay. The substrate p-nitrophenylphosphate (pNPP) was catalyzed by VHHjd8-ALP into p-nitrophenol (pNP). Afterward, the blue-emissive CDs (bCDs) were added. In the presence of pNP, the fluorescent intensity of bCDs can be quenched through an inner-filter effect. The implementation of this sensitivity enhancement strategy does not require additional steps, making it a convenient, time-saving, and effective method for fenitrothion analysis. Moreover, the FIA being developed is undergoing meticulous optimization and will

be thoroughly validated using real samples to ensure its accuracy and practicality.

Materials and methods

Materials and reagents

Fenitrothion standard was purchased from Tanmo Technology Ltd. (Beijing, China). VHHjd8-ALP and coating antigen (Hapten-1-BSA) were prepared and stored in our laboratory (Chen et al., 2021; Liu et al., 2022). Tris(hydroxymethyl)aminomethane (Tris), Tween-20, citric acid, and sodium hydrogen citrate were purchased from Aladdin Chemical Technology Co., Ltd. (Shanghai, China). Urea was supplied by Heowns Biochemical Technology Co., Ltd. (Tianjin, China). The pNPP and dialysis bag (800 Da) were purchased from Yuanye Bio-Technology Co., Ltd. (Shanghai, China). For pretreatment purification, the primary secondary amine (PSA) was obtained from Biocomma Co., Ltd. (Shenzhen, China). The 96 microwell opaque plate and the ELISA plate were purchased from Jingan Biological Co., Ltd. (Shanghai, China).

Buffers

The following buffers and solutions were used in this study: Tris buffer (10 mM, pH 7.4); washing buffer (Tris buffer with 0.05% Tween-20); phosphate-buffered saline (PBS, 10 mM, pH 7.4); PBS with 0.05% Tween-20 (PBST); carbonate buffer (50 mM, pH 9.6); blocking buffer (5% skimmed milk in PBS); and ALP buffer (Tris, 5 mM, pH 9.6, with 2 mM MgCl₂).

Instruments

The morphology characterization of bCDs was performed in the Gene Pulser Xcell electroporator (Bio-Rad, Hercules, CA, United States). The Multiskan MK3 microplate reader was employed for the optical density (OD) value measurement (Thermo-Fisher, Waltham, MA, United States). SpectaMax i3x reader was used to measure fluorescence intensity (Molecular Devices, Sunnyvale, United States). Characterization of bCDs was performed using an FEI Talos F200X microscope (Thermo-Fisher, Hillsboro, OR, United States), a Nicolet IS10 FT-IR Spectrometer (Thermo-Fisher, Waltham, MA, United States), an FLS1000/FSS FL spectrometer (Edinburgh Instruments Ltd., Livingston, UK), and an ESCALAB 250XI electron spectrometer (Thermo Scientific, Waltham, MA, United States).

Preparation of rCDs

The synthesis of bCDs was referred to by Qu et al. (2016) using the hydrothermal method. A mixture of citric acid (1 g) and urea (2 g) was dissolved in N,N-dimethylformamide (10 mL) and then heated for 6 h at 160°C in a Teflon-lined autoclave. The obtained dark product was dialyzed by an 800 Da dialysis bag with deionized water to remove unreacted substances. The bCDs were finally obtained after dialysis and stored at 4°C until used.

Development of FIA

The Hapten-1-BSA was diluted in carbonate buffer (1 $\mu\text{g}/\text{mL}$) and added to an ELISA plate (100 $\mu\text{L}/\text{well}$) kept overnight at 37°C. After coating, the ELISA plate was washed twice with PBST. To block the uncoated sites, a blocking buffer was added (120 $\mu\text{L}/\text{well}$) and incubated for 3 h at 37°C and dried at 37°C for 1 h. A series of fenitrothion solutions (in Tris buffer) were added to the microplate (50 $\mu\text{L}/\text{well}$), followed by the addition of VHHjd8-ALP (in Tris buffer, 50 $\mu\text{L}/\text{well}$). After a 30-min incubation period, the wells were washed five times with a washing buffer. Subsequently, the pNPP substrate (in ALP buffer, 100 $\mu\text{L}/\text{well}$) was added and incubated at 37°C for 30 min, following which 50 μL of bCDs was introduced, and the mixture was then transferred to an opaque plate (100 $\mu\text{L}/\text{well}$). The fluorescence signal of bCDs was measured using an excitation wavelength of 370 nm and an emission wavelength of 470 nm.

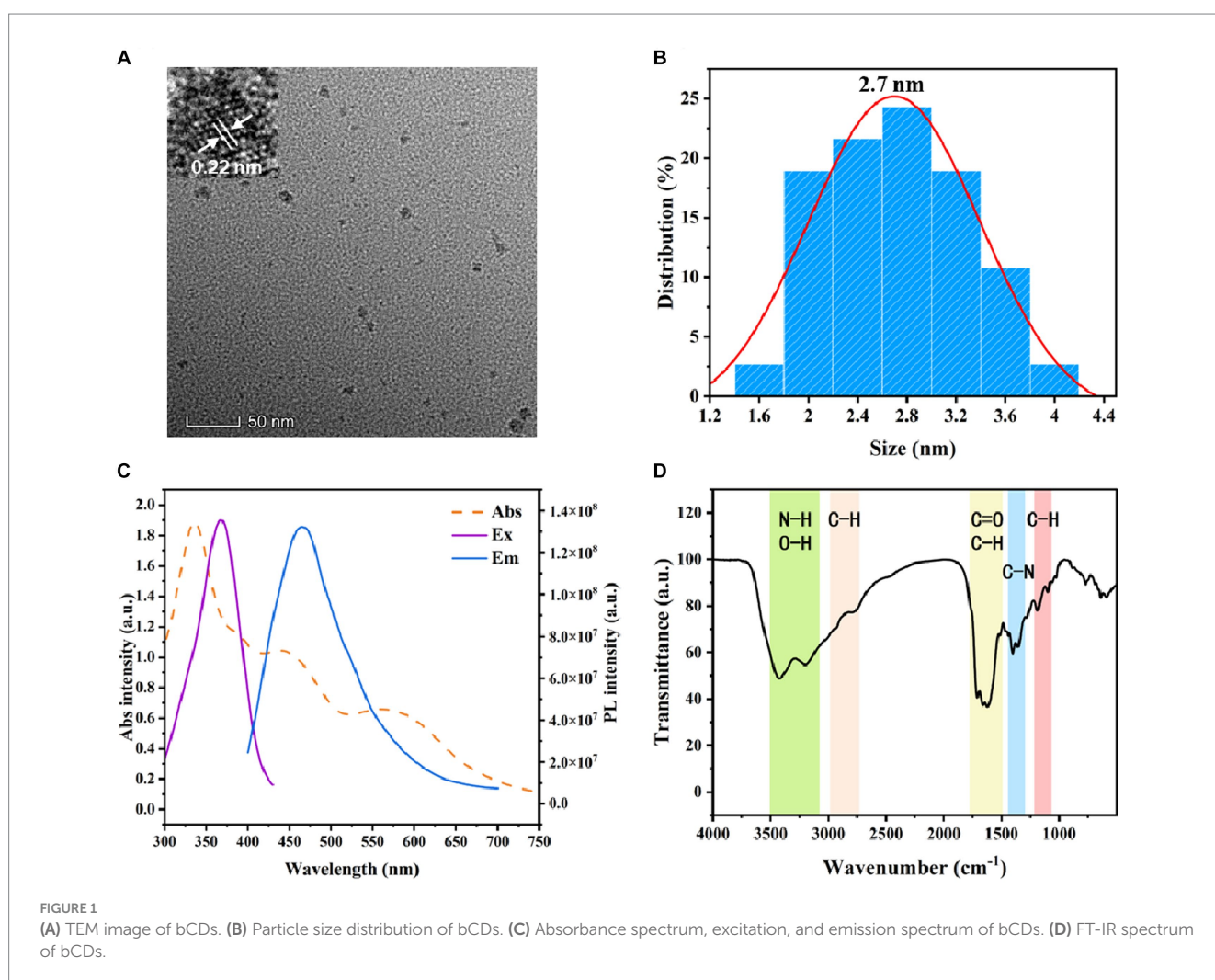
Determination of samples

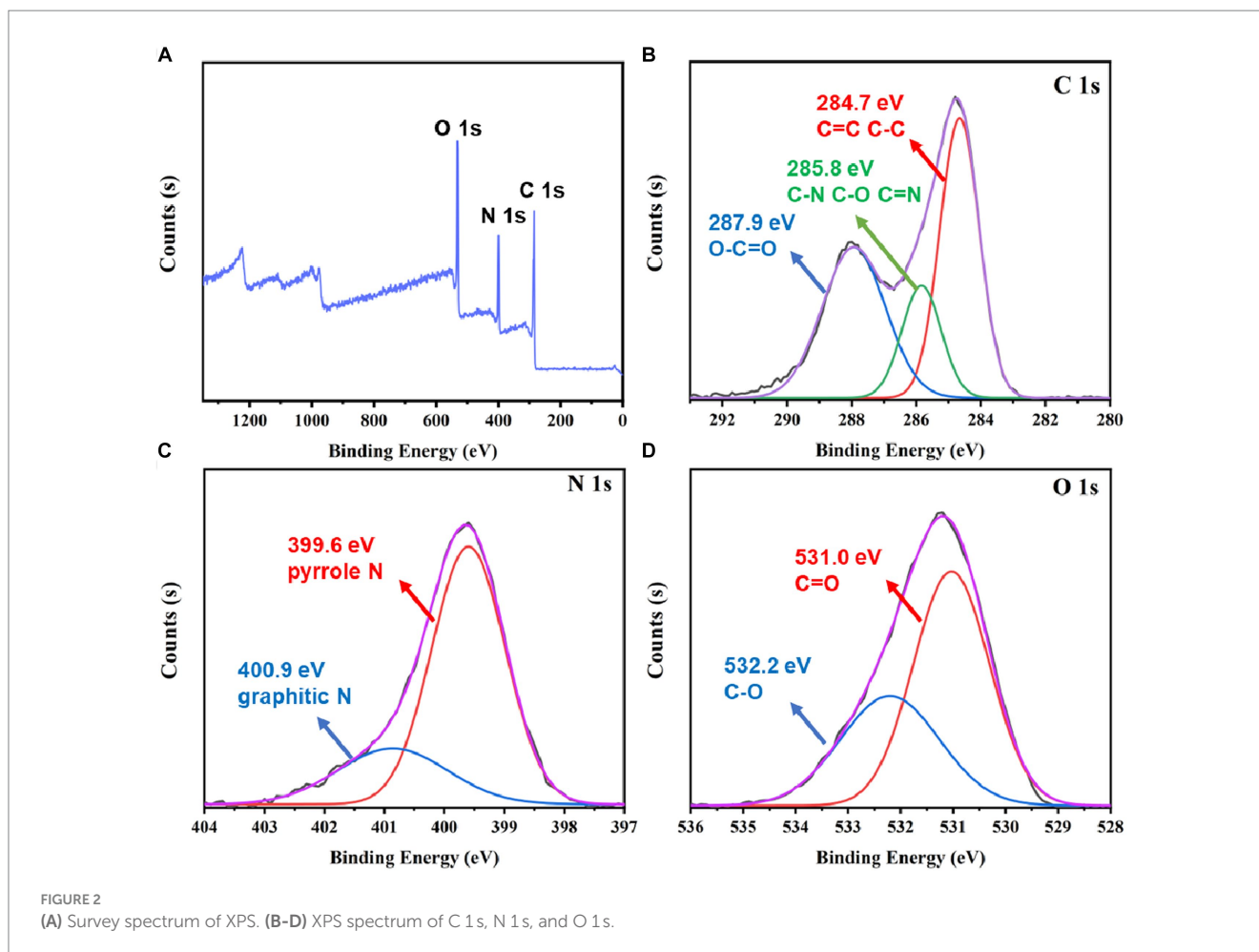
The GC-MS/MS was employed to verify the fenitrothion-free samples (tangerines, lettuces, and Chinese cabbages). The details are described in Supporting Information.

Results and discussion

Identification of bCDs

In a previous study, bifunctional VHHjd8-ALP was prepared for the one-step ELISA of fenitrothion, which was faster than the conventional icELISA. As a typical substrate, pNPP was widely employed for the response of ALP (Sun et al., 2018). However, the sensitivity of pNPP-based ELISA is limited by the strategy of OD value measurement. To overcome this shortcoming, this study synthesized and employed bCDs as a high-response signal probe for sensitivity improvement. Transmission electron microscopy (TEM) was used to characterize the obtained bCDs and revealed well-dispersed nanoparticles, exhibiting a spherical morphology with an interplanar spacing of 0.22 nm (Figure 1A). The size distribution histogram showed the average size of 2.7 nm for bCDs (Figure 1B). The small size of bCDs ensures their effective dispersion in an aqueous solution, enabling their utilization as fluorescent probes for uniform signal response. The optical performance of bCDs (including absorbance spectrum and fluorescence spectrum) was further characterized. As shown in Figure 1C, the UV absorption spectrum of bCDs showed several absorption peaks in the wavelength range of 300–750 nm, while the highest intensity was



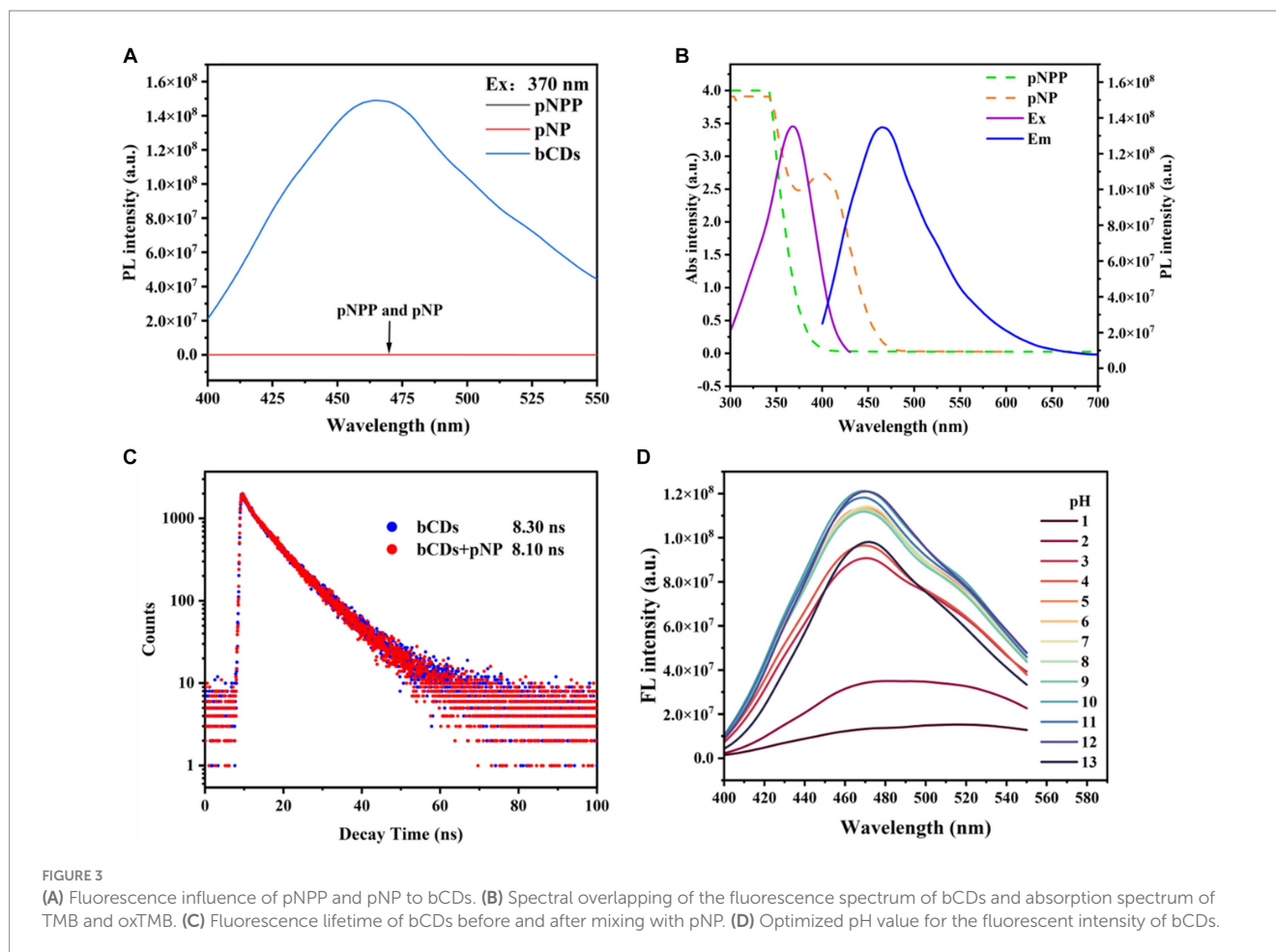


found at 338 nm. Moreover, the excitation spectrum (Ex) showed the strong peak at 370 nm, suggesting that the compound absorbs light most efficiently at this wavelength. Based on the optimized Ex, the emission spectrum was scanned and exhibited the peak centered at 470 nm.

Fourier transform infrared spectroscopy (FT-IR) was employed to analyze the functional groups of bCDs. As depicted in Figure 1D, the existence of wide bands within the range of 3,100–3,500 cm^{-1} confirmed the presence of stretching vibrations associated with O-H or N-H. This observation indicates the presence of -OH or -NH₂ groups. These hydrophilic groups achieved good solubility of bCDs (Qu et al., 2016). A faint peak detected at 2800–3000 cm^{-1} signifies the stretching vibration of saturated C-H bonds (Holá et al., 2017). In the range of 580–1800 cm^{-1} , several absorption peaks were found. The FT-IR spectrum of the bCDs showed characteristic peaks at 1710 cm^{-1} and 1,660 cm^{-1} , indicating the presence of C=O double bond and C-H bond stretching vibrations, respectively (Zhang et al., 2020; Yu et al., 2022). Moreover, the FT-IR spectrum displayed peaks at 1620 cm^{-1} and 1,510 cm^{-1} , suggesting the presence of aromatic groups in bCDs (Zhang et al., 2020). An obvious peak at 1400 cm^{-1} suggested the presence of C-N stretching vibrations, indicating that the amide group exists in bCDs (Yu et al., 2022). The presence of a peak at 1360 cm^{-1} in the FT-IR spectrum was attributed to the bending vibration of the C-H group. The peaks in the range from

1,000 to 1,180 cm^{-1} indicated the C-O groups (Aladesuyi and Oluwafemi, 2023).

To further examine the chemical composition of bCDs, the XPS was employed. Figure 2A shows that the XPS survey spectrum exhibited three element peaks, namely, carbon (C 1s), nitrogen (N 1s), and oxygen (O 1s). To further analyze the functional groups of bCDs, a high-resolution XPS spectrum was employed. Figure 2B shows that the C 1s spectrum decomposed into three peaks. The peaks at 287.9 eV and 284.7 eV demonstrated the existence of O=C-O and C-C (or C=C). Moreover, the peak at 285.8 eV was attributed to the groups of C-N, C-O, or C=N (Zhang et al., 2020). The decomposition of N 1s can be observed in Figure 2C, where it is divided into two distinct peaks at the binding energy of 399.6 eV and 400.9 eV. These peaks correspond to pyrrolic N and graphitic N, respectively (Huo et al., 2021; Wu et al., 2022). The binding energy of O 1s (Figure 2D) can also be deconvoluted into two peaks at the binding energy of 531.0 eV and 532.2 eV, contributed by the bonds of C=O and C-O, respectively (Chen et al., 2020; Zhang et al., 2020). Based on the aforementioned findings, it can be inferred that the bCDs potentially possess a conjugation core consisting of the pyridine and graphitic groups. Additionally, the presence of hydrophilic groups, such as amino and hydroxyl groups on the surface, contributes to the high solubility of bCDs.



Construction of FIA

To verify the feasibility of FIA, several conditions were investigated. The fluorescence spectrum of pNP, pNPP, and bCDs were characterized. As shown in [Figure 3A](#), only bCDs exhibited an obvious emission, and no fluorescence interference was observed for pNP and pNPP on bCDs, indicating the reliable signal output and good signal-to-noise ratio of FIA. To further investigate the quenching mechanism for bCDs, the UV spectrum of pNP and pNPP were measured and compared with the Ex and Em of bCDs. [Figure 3B](#) shows that no absorption peaks were observed for pNPP, while pNP showed an obvious absorption peak at 405 nm, which overlaps the Ex and Em peaks of bCDs. Moreover, the introduction of pNP did not affect the fluorescence lifetime of bCDs ([Figure 3C](#)). Therefore, the inner-filter effect might be the main reason for the fluorescence quenching of bCDs ([Dong et al., 2019](#)). Furthermore, the fluorescence of bCDs was examined across different pH values, revealing that bCDs demonstrated a strong fluorescence intensity within a wide pH range spanning from pH 5 to pH 13, demonstrating superior optics features and stability ([Figure 3D](#)). The pH value of ALP buffer was 9.6, which was suitable for the fluorescent response of bCDs. Therefore, bCDs were added without adjusting the pH value. All the above mentioned results indicated that the FIA system based on phosphate triggered to regulate the intensity of bCDs was feasible.

Development of FIA

Based on the mechanism of fluorescent regulation, the development of FIA was achieved by utilizing bCDs. In the absence of fenitrothion, the VHHjd8-ALP was bound to the microplate after a one-step competitive immune competition. Afterward, the pNPP was catalyzed into pNP through VHHjd8-ALP. Subsequently, the addition of bCDs resulted in the quenching of the fluorescence spectrum through the inner-filter effect, leading to a fluorescent response indicating the presence of fenitrothion ([Scheme 1](#)). To optimize the catalytic activity of VHHjd8-ALP for FIA, the pH value was adjusted and investigated using pNPP as the substrate. [Figure 4A](#) shows that the highest catalytic activity was observed with the pH value of 9.8, which was chosen as the optimized pH to develop FIA. Since the pH value for VHHjd8-ALP matched that of bCDs, no pH adjusting was performed after bCD addition, which was simple and convenient. Furthermore, the coating antigen concentration for the development of FIA was also investigated. [Figure 4B](#) demonstrates that the calibration curve attained optimal sensitivity, as evidenced by the limit of detection (LOD) of 0.77 ng/mL when the coating antigen concentration was set at 1 µg/mL. The calibration curve for FIA was successfully generated under the optimized conditions. The FIA analysis revealed an IC₅₀ value of 16.25 ng/mL, with a limit of detection (LOD) of 0.07 ng/mL ([Figure 5A](#)).

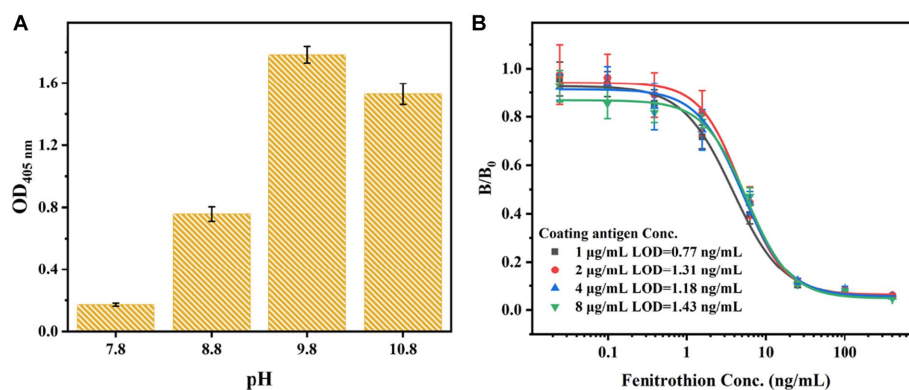


FIGURE 4

(A) pH optimization for the catalytic activity of VHHjd9-ALP. (B) Optimization of coating antigen concentration.

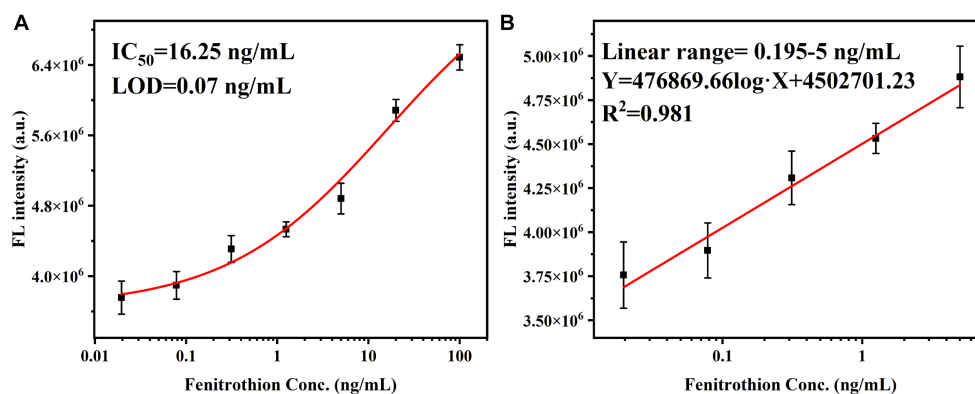


FIGURE 5

(A) Calibration curve and (B) linear range of FIA.

The fluorescent intensity exhibited a strong linear correlation with fenitrothion, with the concentration ranging from 0.195 ng/mL to 5 ng/mL, as evidenced by a high correlation coefficient of $R^2 = 0.981$ (Figure 5B). Compared with conventional pNPP-based one-step icELISA (Figure 4B), the developed FIA exhibited 11-fold improvement. Furthermore, the strategy of enhancing sensitivity necessitates no intricate methodologies, rendering it straightforward, convenient, and cost-effective.

Recovery test

Following the extraction and purification procedures, the extracting solutions were subsequently diluted using Tris buffer. Previous research has demonstrated that a 20-fold dilution effectively eliminates any matrix effect (Chen et al., 2022). To assess the accuracy of the developed FIA, a recovery test was conducted, and the results are summarized in Table 1. The recoveries achieved through FIA ranged from 81.8% to 119%, while those obtained through GC-MS/MS ranged from 86.5% to 116%. The coefficient of variances (CVs) for FIA ranged from 7% to 13.6%, and for GC-MS/MS, the CVs ranged from 4.3% to 11.6%. The results obtained from

FIA exhibited a high level of agreement with those obtained from GC-MS/MS, indicating the accuracy and practicality of the developed FIA method.

Conclusion

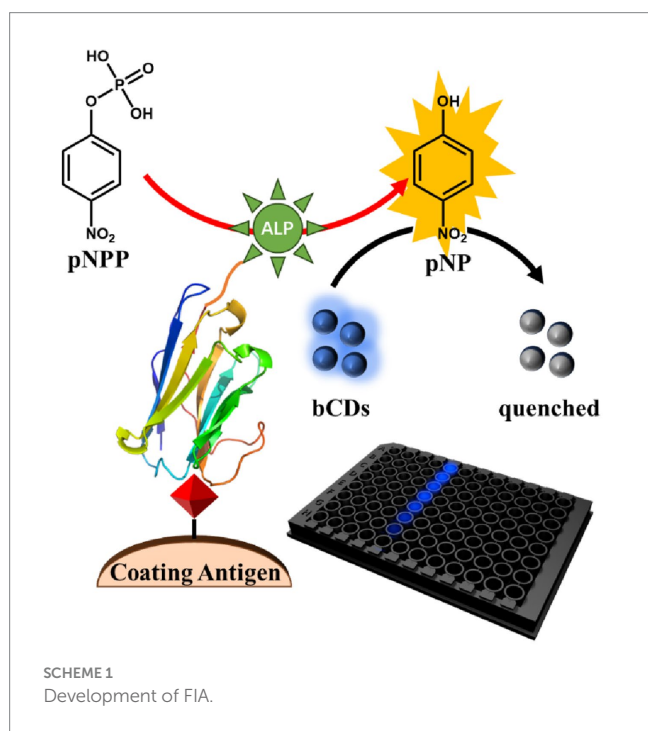
This study developed a simple FIA for sensitive detection of fenitrothion. The synthesized bCDs were used as a fluorescent probe for sensitivity improvement. After conducting a one-step competitive immunoassay, the VHHjd8-ALP fusion protein, upon binding to the microplate, catalyzed the conversion of pNPP into pNP; the latter can quench the intensity of bCDs through the inner-filter effect. After condition optimization, a high fluorescent response immunoassay was finally developed. Furthermore, in comparison to the conventional pNPP-based one-step icELISA, the developed FIA demonstrated a remarkable 11-fold enhancement. Furthermore, the approach to enhancing sensitivity does not require complex methodologies, making it simple, convenient, and economical. The recovery test served as confirmation that the developed FIA was both practical and accurate, establishing it as an exceptional method for rapidly and sensitively detecting fenitrothion in food samples.

TABLE 1 Recovery of fenitrothion from spiked food samples by proposed FIA ($n = 3$).

Sample	Spiked (ng/g)	FIA			GC-MS/MS		
		Measured Mean \pm SD ^a (ng/g)	Recovery (%)	CV ^b (%)	Measured Mean \pm SD (ng/g)	Recovery (%)	CV (%)
Chinese cabbage	2.0	1.6 \pm 0.2	81.8	11.5	1.85 \pm 0.2	92.5	10.8
	10.0	8.2 \pm 0.8	82	9.8	10.34 \pm 0.6	103.4	5.8
	50.0	57.8 \pm 4.7	115.7	8.1	51.31 \pm 3.2	102.6	6.2
Lettuce	2.0	2 \pm 0.2	98.3	11.3	2.15 \pm 0.2	107.5	9.3
	10.0	11.2 \pm 1.4	112.3	12.6	9.47 \pm 1	94.7	10.6
	50.0	56.6 \pm 7.1	113.2	12.6	56.95 \pm 3.9	113.9	6.9
Tangerine	2.0	1.9 \pm 0.3	96.5	13.6	1.73 \pm 0.2	86.5	11.6
	10.0	11.9 \pm 0.8	119	7	11.6 \pm 0.5	116	4.3
	50.0	53.8 \pm 3.9	107.6	7.2	52.77 \pm 3.2	105.6	6.1

^aSD, standard deviation.

^bCV, coefficient of variance, which was obtained from intra-assay.



Z-LX: Conceptualization, Supervision, Writing – review & editing.
HW: Conceptualization, Supervision, Writing – review & editing.

Funding

The author(s) declare financial support was received for the research, authorship, and/or publication of this article. This work was supported by Guangdong Basic and Applied Basic Research Foundation (2021A1515110513), 2023 Natural Science Youth Project of Zhaoqing University (QN202335), the Science Project of Department of Education of Guangdong Province of China (2020ZDZX2044, 2023KTSCX158), the Science and Technology Planning Project of Zhaoqing City of Guangdong Province of China (2021N023, 2021SN007), Central Public-interest Scientific Institution Basal Research Fund (1630112023006).

Conflict of interest

The authors declare that the research was conducted in the absence of any commercial or financial relationships that could be construed as a potential conflict of interest.

Data availability statement

The original contributions presented in the study are included in the article/[Supplementary material](#), further inquiries can be directed to the corresponding authors.

Author contributions

Z-JC: Data curation, Methodology, Writing – original draft. A-JH: Data curation, Methodology, Writing – original draft. X-XD: Methodology, Validation, Writing – review & editing. Y-FZ: Data curation, Methodology, Writing – original draft. LZ: Writing – review & editing, Supervision. LL: Writing – review & editing, Methodology.

Publisher's note

All claims expressed in this article are solely those of the authors and do not necessarily represent those of their affiliated organizations, or those of the publisher, the editors and the reviewers. Any product that may be evaluated in this article, or claim that may be made by its manufacturer, is not guaranteed or endorsed by the publisher.

Supplementary material

The Supplementary material for this article can be found online at: <https://www.frontiersin.org/articles/10.3389/fsufs.2023.1320931/full#supplementary-material>

References

- Abdel-Ghany, R., Mohammed, E., Anis, S., and Barakat, W. (2016). Impact of exposure to Fenitrothion on vital organs in rats. *J. Toxicol.* 2016, 1–18. doi: 10.1155/2016/5609734
- Aladesuyi, O. A., and Oluwafemi, O. S. (2023). Synthesis of N, S co-doped carbon quantum dots (N,S-CQDs) for sensitive and selective determination of mercury (Hg²⁺) in *Oreochromis niloticus* (Tilapia fish). *Inorg. Chem. Commun.* 153:110843. doi: 10.1016/j.inoche.2023.110843
- Chen, Z. J., Huang, Z. C., Huang, S., Zhao, J. L., Sun, Y. M., Xu, Z. L., et al. (2021). Effect of proteins on the oxidase-like activity of CeO₂ nanozymes for immunoassays. *Analyst* 146, 864–873. doi: 10.1039/d0an01755h
- Chen, Y. Q., Sun, X. B., Wang, X. Y., Pan, W., Yu, G. F., and Wang, J. P. (2020). Carbon dots with red emission for bioimaging of fungal cells and detecting Hg²⁺ and ziram in aqueous solution. *Spectrochim. Acta A* 233:118230. doi: 10.1016/j.saa.2020.118230
- Chen, Z. J., Zhang, Y. F., Chen, J. L., Lin, Z. S., Wu, M. F., Shen, Y. D., et al. (2022). Production and characterization of biotinylated anti-fenitrothion nanobodies and development of sensitive fluoroimmunoassay. *J. Agric. Food Chem.* 70, 4102–4111. doi: 10.1021/acs.jafc.2c00826
- Delnavaz, E., Amjadi, M., and Farajzadeh, M. A. (2023). Metal-organic framework with dual-loading of nickel/nitrogen-doped carbon dots and magnetic nanoparticles for fluorescence detection of fenitrothion in food samples. *J. Food Compos. Anal.* 115:104873. doi: 10.1016/j.jfca.2022.104873
- Dong, B. L., Li, H. F., Mujtaba Mari, G., Yu, X. Z., Yu, W. B., Wen, K., et al. (2019). Fluorescence immunoassay based on the inner-filter effect of carbon dots for highly sensitive amantadine detection in foodstuffs. *Food Chem.* 294, 347–354. doi: 10.1016/j.foodchem.2019.05.082
- Faria, M., Bellot, M., Bedrossiantz, J., Ramirez, J., Prats, E., Garcia-Reyero, N., et al. (2022). Environmental levels of carbaryl impair zebrafish larvae behaviour: the potential role of ADRA2B and HTR2B. *J. Hazard. Mater.* 431:128563. doi: 10.1016/j.jhazmat.2022.128563
- Galal, A. A. A., Ramadan, R. A., Metwally, M. M. M., and El-Sheikh, S. M. A. (2019). Protective effect of N-acetylcysteine on fenitrothion-induced toxicity: the antioxidant status and metabolizing enzymes expression in rats. *Ecotoxicol. Environ. Saf.* 171, 502–510. doi: 10.1016/j.ecoenv.2019.01.004
- Gnanguenon, V., Agossa, F. R., Badirou, K., Govoetchan, R., Anagonou, R., Oke-Agbo, F., et al. (2015). Malaria vectors resistance to insecticides in Benin: current trends and mechanisms involved. *Parasit. Vectors* 8:223. doi: 10.1186/s13071-015-0833-2
- Han, J., Zhang, Y., Chen, Z., Zhang, A., and Shi, X. (2023). Synergistic effect of nitrogen and sulfur co-doped holey graphene for sensitive fenitrothion detection supported by DFT study. *Microchem. J.* 193:109218. doi: 10.1016/j.microc.2023.109218
- Holá, K., Sudolská, M., Kalytchuk, S., Nachtigallová, D., Rogach, A. L., Otyepka, M., et al. (2017). Graphitic nitrogen triggers red fluorescence in carbon dots. *ACS Nano* 11, 12402–12410. doi: 10.1021/acsnano.7b06399
- Huo, X., Shen, H., Liu, R., and Shao, J. (2021). Solvent effects on fluorescence properties of carbon dots: implications for multicolor imaging. *ACS Omega* 6, 26499–26508. doi: 10.1021/acsomega.1c03731
- Kang, H. S., Kim, M., Kim, E. J., and Choe, W. (2020). Determination of 66 pesticide residues in livestock products using QuEChERS and GC-MS/MS. *Food Sci. Biotechnol.* 29, 1573–1586. doi: 10.1007/s10068-020-00798-4
- Lee, C., Kwon, W., Beack, S., Lee, D., Park, Y., Kim, H., et al. (2016). Biodegradable nitrogen-doped carbon nanodots for non-invasive photoacoustic imaging and photothermal therapy. *Theranostics* 6, 2196–2208. doi: 10.7150/thno.16923
- Li, W., Ma, L., Shi, Y., Wang, J., Yin, J., Wang, D., et al. (2023). Meiosis-mediated reproductive toxicity by fenitrothion in *Caenorhabditis elegans* from metabolomic perspective. *Ecotoxicol. Environ. Saf.* 253:114680. doi: 10.1016/j.ecoenv.2023.114680
- Lin, X., Xiong, M., Zhang, J., He, C., Ma, X., Zhang, H., et al. (2021). Carbon dots based on natural resources: synthesis and applications in sensors. *Microchem. J.* 160:105604. doi: 10.1016/j.microc.2020.105604
- Liu, M. L., Zeng, X., Deng, H., Wang, Y., Zhang, Y. F., Shen, Y. D., et al. (2022). Phosphate-triggered ratiometric multicolor immunosensor based on nanobody-alkaline phosphatase fusion protein for sensitive detection of fenitrothion. *Sensor. Actuat. B Chem.* 373:132734. doi: 10.1016/j.snb.2022.132734
- Luo, P. G., Sahu, S., Yang, S., Sonkar, S. K., Wang, J., Wang, H., et al. (2013). Carbon "quantum" dots for optical bioimaging. *J. Mater. Chem. B* 1, 2116–2127. doi: 10.1039/c3tb00018d
- Pedroso, T. M. A., Benvindo-Souza, M., de Araújo Nascimento, F., Woch, J., Dos Reis, F. G., de Melo, E., et al. (2022). Cancer and occupational exposure to pesticides: a bibliometric study of the past 10 years. *Environ. Sci. Pollut. Res.* 29, 17464–17475. doi: 10.1007/s11356-021-17031-2
- Qu, S. N., Zhou, D., Li, D., Ji, W. Y., Jing, P. T., Han, D., et al. (2016). Toward efficient orange emissive carbon nanodots through conjugated sp²-domain controlling and surface charges engineering. *Adv. Mater.* 28, 3516–3521. doi: 10.1002/adma.201504891
- Sun, J., Zhao, J., Bao, X., Wang, Q., and Yang, X. (2018). Alkaline phosphatase assay based on the chromogenic interaction of Diethanolamine with 4-aminophenol. *Anal. Chem.* 90, 6339–6345. doi: 10.1021/acs.analchem.8b01371
- Ulusoy, H., Köseoğlu, K., Kabir, A., Ulusoy, S., and Locatelli, M. (2020). Fabric phase sorptive extraction followed by HPLC-PDA detection for the monitoring of pirimicarb and fenitrothion pesticide residues. *Microchim. Acta* 187:337. doi: 10.1007/s00604-020-04306-7
- Wang, Y., Liu, X., Chen, C., Chen, Y., Li, Y., Ye, H., et al. (2022). Magnetic Nanorobots as maneuverable immunoassay probes for automated and efficient enzyme linked immunosorbent assay. *ACS Nano* 16, 180–191. doi: 10.1021/acsnano.1c05267
- Wu, Z. L., Xiong, Z. K., Liu, R., He, C. S., Liu, Y., Pan, Z. C., et al. (2022). Pivotal roles of N-doped carbon shell and hollow structure in nanoreactor with spatial confined co species in peroxymonosulfate activation: obstructing metal leaching and enhancing catalytic stability. *J. Hazard. Mater.* 427:128204. doi: 10.1016/j.jhazmat.2021.128204
- Yang, N., Wang, P., Xue, C. Y., Sun, J., Mao, H. P., and Oppong, P. K. (2018). A portable detection method for organophosphorus and carbamates pesticide residues based on multilayer paper chip. *J. Food Process Eng.* 41:e12867. doi: 10.1111/jfpe.12867
- Yi, K. Y., Zhang, X. T., and Zhang, L. (2020). Eu³⁺@metal-organic frameworks encapsulating carbon dots as ratiometric fluorescent probes for rapid recognition of anthrax spore biomarker. *Sci. Total Environ.* 743:140692. doi: 10.1016/j.scitotenv.2020.140692
- Yu, M., Zhang, H., Liu, Y. N., Zhang, Y. L., Shang, M. H., Wang, L., et al. (2022). A colorimetric and fluorescent dual-readout probe based on red emission carbon dots for nitrite detection in meat products. *Food Chem.* 374:131768. doi: 10.1016/j.foodchem.2021.131768
- Zhang, X. Q., Chen, C. Y., Peng, D. P., Zhou, Y. Z., Zhuang, J. L., Zhang, X. J., et al. (2020). pH-responsive carbon dots with red emission for real-time and visual detection of amines. *J. Mater. Chem. C* 8, 11563–11571. doi: 10.1039/d0tc02597f
- Zhu, Z. J., Zhai, Y. L., Li, Z. H., Zhu, P. Y., Mao, S., Zhu, C. Z., et al. (2019). Red carbon dots: optical property regulations and applications. *Mater. Today* 30, 52–79. doi: 10.1016/j.mattod.2019.05.003